Author Manuscript

Author Manuscript

Author Manuscript

Author Manuscript

HHS Public Access

Author manuscript

J Bone Miner Metab. Author manuscript; available in PMC 2019 January 08.

Published in final edited form as:

J Bone Miner Metab. 2018 January ; 36(1): 64–72. doi:10.1007/s00774-017-0820-0.

Bhlha9 regulates apical ectodermal ridge formation during limb development

Kensuke Kataoka[#1], **Takahide Matsushima**[#1], **Yoshiaki Ito**[1], **Tempei Sato**[1], **Shigetoshi Yokoyama**[2], and **Hiroshi Asahara**[1,2]

[1]Department of Systems BioMedicine, Tokyo Medical and Dental University, 1-5-45 Yushima, Bunkyo-ku, Tokyo 113-8510, Japan

[2]Department of Systems Biomedicine, National Research Institute for Child Health and Development, 2-10-1, Okura, Setagaya, Tokyo 157-0074, Japan

[#] These authors contributed equally to this work.

Abstract

Split hand/foot malformation (SHFM) and SHFM combined with long-bone deficiency (SHFLD) are congenital dysgeneses of the limb. Although six different loci/mutations (SHFM1–SHFM6) have been found from studies on families with SHFM, the causes and associated pathogenic mechanisms for a large number of patients remain unidentified. On the basis of the identification of a duplicated gene region involving *BHLHA9* in some affected families, *BHLHA9* was identified as a novel SHFM/SHFLD-related gene. Although *Bhlha9* is predicted to participate in limb development as a transcription factor, its precise function is unclear. Therefore, to study its physiological function, we generated a *Bhlha9*-knockout mouse and investigated gene expression and the associated phenotype in the limb bud. *Bhlha9*-knockout mice showed syndactyly and poliosis in the limb. Moreover, some apical ectodermal ridge (AER) formation related genes, including *Trp63*, exhibited an aberrant expression pattern in the limb bud of *Bhlha9*-knockout mice; *TP63* (*Trp63*) was regulated by *Bhlha9* on the basis of in vitro analysis. These observations suggest that *Bhlha9* regulates AER formation during limb/finger development by regulating the expression of some AER-formation-related genes and abnormal expression of *Bhlha9* leads to SHFM and SHFLD via dysregulation of AER formation and associated gene expression.

Keywords

Split hand/foot malformation; Split hand/ foot malformation combined with long-bone deficiency; *Bhlha9*

Corresponding author: Hiroshi Asahara, asahara.syst@tmd.ac.jp.

Conflict of interest

The authors declare that they have no conflict of interest.

Author Manuscript Author Manuscript Author Manuscript Author Manuscript

Introduction

Split hand/foot malformation (SHFM) is a form of limb dysgenesis. Its phenotype is extremely variable between and within families, ranging from ectrodactyly and syndactyly to monodactyly. Six loci/mutations (SHFM1– SHFM6) were found to be associated with human nonsyndromic SHFM [1]. Representatively, mutations in *TP63* (*Trp63*), encoding a homologue of the tumor suppressor p53, were identified as a causative factor for SHFM4 [2, 3]. *TP63* (*Trp63*) RNA is transcribed from two different transcription start sites, yielding both transactivating (TA-*p63*) and nontransactivating (ΔN-*p63*) isotypes. The dominant negative isotype ΔN-*p63* is specifically expressed in the apical ectodermal ridge (AER) and is thought to function as a transcription factor that is involved in AER maintenance [4]. In fact, the forelimbs of *Trp63*-knockout mice are severely malformed, lacking the radius and autopod [5, 6]. However, the disease-associated genes and pathogenic mechanisms in a large number of nonsyndromic SHFM cases, including SHFM combined with long-bone deficiency (SHFLD), remain unidentified.

Recent reports have indicated that 17p13.3 duplications should be considered the commonest cause of SHFM/ SHFLD [7–14]. In particular, Klopocki et al. [9] scrutinized the minimal critical region (11.8 kb) by analyzing 17 families with 17p13.3 duplications, and identified *BHLHA9* [which encodes basic helix–loop–helix (bHLH) family member A9] as a novel SHFM/SHFLD-related gene.

BHLHA9 encodes a member of the bHLH transcription factor family that is predicted to participate in limb development as a transcription factor. Knockdown of *Bhlha9* in zebrafish results in severely truncated pectoral fins [9]. Furthermore, *Bhlha9*-knockout mice exhibit various degrees of syndactyly [15]. In addition, Malik et al. [16] demonstrated that three missense mutations affecting the highly conserved DNA-binding domain of *BHLHA9* are associated with mesoaxial synostotic syndactyly, Malik–Percin type. From these studies, it appears that *Bhlha9* is a key molecular player in limb and finger development. However, the precise function of *Bhlha9* as a transcription factor is unknown, and its downstream genes have not been identified. To elucidate the physiological function of *Bhlha9*, we generated knockout mice and investigated their phenotypes and gene expression patterns in the limb bud.

Materials and Methods

Generation of *Bhlha9* Knockout Mice

All animal experiments were performed according to protocols approved by the institutional animal care and use committees of the National Institute for Child Health and Development and Tokyo Medical and Dental University. A vector was constructed for replacement of the endogenous *Bhlha9* locus with the *Venus-Cre* and PGK-Neo cassette via homologous recombination in embryonic stem cells (Fig. S1a). Through PCR, 5′ and 3′ sequences flanking the endogenous *Bhlha9* locus were amplified from a C57BL/6 genomic bacterial artificial chromosome clone (BACPAC Resource Center). These homology arms were cloned into a vector harboring both a neomycin resistance cassette for positive selection and a diphtheria toxin A encoding gene for negative selection. The targeting vector was

Author Manuscript Author Manuscript Author Manuscript Author Manuscript

linearized and electroporated into TT2F embryonic stem cells. Recombinant embryonic stem cell clones were isolated after culturing in medium containing G418 antibiotic (Invitrogen) and were screened for proper integration by Southern blotting with use of a 5′ probe (Fig. S1b). The resulting chimeric offspring were crossed with C57BL/6 mice, and germline transmission was confirmed by PCR (Fig. S1c). The mouse genotypes were determined by PCR with use of tail DNA as the template and the following primers: T1, 5′-TGAAGCTG TGAGACCAGGACA-3′: T2, 5′-GGCCGTGACACTCCA GGT-3′; and T3, 5′-GTTCTGCTGGTAGTGGTCGG-3′.

In Situ Hybridization

In situ hybridization on whole mounts and sections was performed as previously described [17]. Briefly, tissues were embedded in optimal cutting temperature compound (Sakura Finetek) and ash-frozen in liquid nitrogen. Specimens were sectioned to 16μm with use of a CM3050 S cryostat (Leica) and hybridized with digoxigenin-labeled antisense RNA probes. Detailed descriptions of the RNA probes are available from the authors on request.

Histological Analysis

For histological analysis of the interdigit, the forelimbs were harvested from adult mice and fixed with 4% paraformaldehyde in phosphate-buffered saline at 4 °C overnight. Tissues were dehydrated, embedded in paraffin, and sectioned; these sections were stained with hematoxylin and eosin (Wako). Skeleton specimens from 3-month-old adult *Bhlha9*-knockout and wild-type littermate control mice were stained with Alcian blue/alizarin red as previously described [18]. The length of the limb skeleton was measured by analysis of an image obtained with an SZX16 stereoscopic microscope (Olympus).

RNA Isolation and Quantitative Real-Time PCR

Total RNA was isolated from limb buds and cells with use ISOGEN (Nippon Gene), and was reverse-transcribed with a ReverTraAce kit (Toyobo) according to the manufacturer's instructions. Complementary DNA was used for quantitative real-time PCR (qPCR), and qPCR was performed with use of Thunderbird SYBR mix (Toyobo). β-*Actin* expression served as the control for messenger RNA expression. Changes in gene expression were quantified by the ΔΔCT method. The primer sequences for qPCR are described in Table S1.

Microarray Analysis

RNA samples were obtained from the whole limb bud of embryonic day 10.5 (E10.5) wild-type and *Bhlha9*-knockout embryos, as described already. Total RNA (200 ng) was reverse-transcribed and biotinylated with use of a GeneChip 3′ IVT Express kit (Affymetrix). Finally, the complementary RNA was hydrolyzed and hybridized to a GeneChip Mouse Genome 430 2.0 array (Affymetrix). The microarray data were summarized with use of the MAS 5.0 method. We applied the following thresholds for data analysis: signal intensity greater than 100, detection call present, and signal intensity upregulated or downregulated more than twofold compared with that of the control. Microarray data are shown in Table S2 and were deposited in the Gene Expression Omnibus repository under accession number GSE81223.

Author Manuscript Author Manuscript Author Manuscript Author Manuscript

Plasmid constriction

To prepare pMIGR-3×FLAG-BHLHA9, complementary DNA encoding full-length human BHLHA9 was artificially constructed (GenScript) and cloned into pMIGR (Addgene). Each 4-kb upstream region of the TA-*p63* and ΔN-*p63* first protein coding exon was cloned from the A549 genome and subcloned into a promoterless pNL1.1 nanoluciferase vector to be used for luciferase assays. The plasmids were sequenced to verify the absence of mutations.

Cell culture and Luciferase assay

HeLa cells and PLAT-E cells were cultured in 10% fetal bovine serum–Dulbecco's modified Eagle's medium containing 1% penicillin–streptomycin (all from Sigma-Aldrich). PLAT-E cells were transfected with the pMIGR construct (as a control) or the pMIGR-3×FLAG-BHLHA9 construct with use of FugeneHD (Promega). Forty-eight hours later, the media were collected, filtered, and transferred to the HeLa stable cell line in a medium containing puromycin (1μg/ml). Control or 3×FLAG-BHLHA9-expressing HeLa stable cells were cotransfected with each *TP63* promoter–nanoluciferase reporter gene construct and the pGL4.13 luciferase construct (for normalization; Promega) with use of Fugene HD (Promega). Cell extracts were prepared 48 h after transfection, and luciferase activity was measured with a Nano-Glo dual-luciferase reporter assay system (Promega).

Results

Bhlha9 expression in mouse limb buds

First, we assessed endogenous *Bhlha9* expression in the limb buds of mouse embryos. Previous studies using a *LacZ* reporter system showed that *Bhlha9* is expressed in the ectodermal region of the digit near the AER on embryonic days 10–15 [15]; however, a time-dependent change in endogenous *Bhlha9* expression had not been demonstrated. Therefore, we investigated endogenous *Bhlha9* expression in the limb bud using in situ hybridization with whole mounts and sections from different stages of embryonic development.

Endogenous *Bhlha9* expression in the limb bud was clearly detected on both the dorsal side and the ventral side of the autopod surface, covering the progress zone near the AER, at E10.5 to embryonic day 11.5 (E11.5) (Fig. 1, panels a, b, d, e, g, h). In contrast, *Bhlha9* expression in the limb bud was undetectable at embryonic day 12.5 (E12.5) in whole mounts, and was barely visible in tissue sections (Fig. 1, panels c, f, i). We were unable to perform this technique at later developmental stages (data not shown). This observation was confirmed with use of limb bud RNA and qPCR analysis (Fig. 1j). From these results, we estimated that *Bhlha9* potentially functions during early embryonic stages (E10.5–E11.5) but not during later developmental stages.

Bhlha9-knockout mouse phenotype

To study the physiological function of *Bhlha9*, we generated the *Bhlha9*-knockout mouse and investigated its phenotype. Our *Bhlha9*-knockout mouse was constructed by replacement of endogenous *Bhlha9* with *Venus-Cre* (Fig. S1a). Unfortunately, Venus-Cre protein expression in *Bhlha9*-knockout mouse limb bud was not detectable by general

Author Manuscript Author Manuscript Author Manuscript Author Manuscript

biological analyses, although genome mutation was confirmed by Southern blotting and PCR analysis (Fig. S1b, c).

As stated in a previous report, the *Bhlha9*-knockout mouse showed syndactyly in the forelimb bud (Fig. 2a) [15]. Furthermore, we also found the new phenotype that the *Bhlha9*-knockout mouse frequently showed poliosis in the hindlimb finger (Fig. 2b). Neither phenotype was observed in heterozygous mice. Next, we used the forelimb to investigate the nature of the syndactyly and the involvement of soft and/or skeletal tissues in it. We performed alizarin red and alcian blue staining of bone and cartilage respectively (Fig. 2c). We found no apparent skeletal abnormalities in the hand plates or arms; hence, the mechanism did not involve defects in skeletal patterning. To clarify the detailed phenotype of the *Bhlha9*-knockout mice, we investigated their interdigital webbing (Fig. 2d). The fused interdigital webbing in adult *Bhlha9*-knockout mice (3 months old) exhibited a large number of hematoxylin-positive cells by hematoxylin and eosin staining. This result shows a disruption of cell death in the *Bhlha9*-knockout mouse interdigital webbing tissue, as stated in previous reports [15].

Gene expression in the *Bhlha9*-knockout mouse limb bud

The *Bhlha9*-knockout mouse exhibited abnormal limb development and a disruption of cell death in interdigital webbing tissue (Fig. 2) [15]; however, the molecular mechanism of this phenotype remains unknown. Hence, to investigate the physiological function of BHLHA9 as a transcription factor, we performed global gene expression analysis using limb bud RNA. Since *Bhlha9* expression was predominant at the E10.5 embryonic stage (Fig. 1), we used E10.5 limb bud RNA for this experiment.

No apparent changes in the expression of major programmed-cell-death-related genes were found in *Bhlha9*-knockout mouse limb buds by microarray analysis. However, several genes related to limb development, including *Trp63*, were highly upregulated in the limb bud of *Bhlha9*-knockout mice (Fig. 3a, Table S2). Differential expression of selected genes was confirmed by qPCR analysis. It was evident that *Trp63* and *Fgf8*, which is a gene downstream of *Trp63* and a representative inhibitor of interdigital cell apoptosis, were upregulated in the limb bud of *Bhlha9*-knockout mice (Fig. 3b). In contrast, the expression of syndactyly-related genes was unaltered. In addition, *Trp63* and *Fgf8* overexpression in *Bhlha9*-knockout mouse limb buds was not confirmed at embryonic day 13.5 (E13.5) (Fig. S2). These results indicate that *Bhlha9* transiently regulates the expression of *Trp63* and its downstream genes during embryonic stages E10.5–E11.5, but not at later developmental stages.

Bhlha9 regulates *TP63* (*Trp63*) and *Fgf8* expression

TP63 (*Trp63*) and *Fgf8* are expressed in the AER, and serve as key molecular modulators of limb development [5, 6, 19, 20]. On the basis of gene expression analysis, abnormal expression of these genes was confirmed in E10.5 limb buds of *Bhlha9*-knockout mice. Thus, we investigated the expression patterns of *Trp63* and *Fgf8* in E10.5 *Bhlha9*-knockout mouse limb buds using in situ hybridization with whole mounts and sections.

Author Manuscript Author Manuscript Author Manuscript Author Manuscript

Trp63 and *Fgf8* were clearly detected in the AER of wild-type mouse limb buds (Fig. 4a, b). However, in the AER of *Bhlha9*-knockout mouse limb buds, the regions that expressed *Trp63* and *Fgf8* were expanded to the progress zone (Fig. 4c, d). The wild-type mouse AER also had a characteristic convex structure; however, this characteristic shape was not detected in the *Bhlha9*-knockout mouse AER (Fig. 4b, d).

On the basis of in situ hybridization analysis using whole mounts and sections, we hypothesized that *Bhlha9* regulates the expression of *Trp63* in the progress zone. We validated this contention by in vitro analysis. *TP63* (*Trp63*) RNA is transcribed from two different transcription start sites, yielding the TA-*p63* and ΔN-*p63* isotypes. Especially, the dominant-negative isoform (ΔN-*p63*) is found to be specifically expressed in the AER, and is thought to function as a transcription factor that is involved in AER maintenance [5]. First, we constructed TA-*p63* and ΔN-*p63* promoter driven luciferase reporter genes to investigate the effect of *Bhlha9* on the transcription of these genes (Fig. 5a). We subcloned the 4-kb upstream regions of the TA-*p63* and ΔN-*p63* first protein coding exons, which include several E-box domains that are recognized by the bHLH transcription factor protein family. We also used the HeLa cell line for in vitro analysis and prepared control and 3×FLAG-BHLHA9-expressing HeLa stable cells using retrovirus systems (Fig. 5b), because these cells can be used to detect the expression of endogenous *TP63* (data not shown). Luciferase assays using TA-*p63* and ΔN-*p63* promoter driven luciferase reporter genes resulted in low luciferase activity in 3×FLAG-BHLHA9-expressing HeLa stable cells as compared with that in control HeLa stable cells (Fig. 5c). Furthermore, endogenous *TP63* expression, including TA-*p63* and ΔN-*p63* expression, was downregulated in 3×FLAG-BHLHA9-expressing HeLa stable cells (Fig. 5d). Both results suggest that *Bhlha9* directly sup- presses the expression of *TP63* (*Trp63*), including TA-*p63* and ΔN-*p63*. Our findings suggest that *Bhlha9* maintains the AER formation by regulating *TP63* (*Trp63*) expression and its downstream genes including *Fgf8*, which is known as an inhibitor of interdigital cell apoptosis, in the progress zone. The results suggest that this occurs at an earlier embryonic stage than the interdigital apoptosis stage, and that this function might contribute to finger morphogenesis.

Discussion

We have reported for the first time that endogenous *Bhlha9* was prominently expressed at embryonic stage E10.5 on both the dorsal surface and the ventral surface, covering the progress zone near the AER (Fig. 1). Moreover, abnormalities in limb development, specifically, syndactyly in the forelimb bud and poliosis in the hindlimb finger, were found in *Bhlha9*-knockout mice (Fig. 2). On the basis of these observations, we hypothesized that BHLHA9 acts as a transcription factor during an early embryonic stage rather than during the interdigital cell apoptosis stage. As such, we determined that two AER-formation-related genes, *Trp63* and *Fgf8*, exhibit transient aberrant expression patterns in *Bhlha9*-knockout mouse limb buds at E10.5, but not at E13.5 (Figs. 3, S2). It has been reported that the AER formation regresses after E12.5 [21]. Previous reports and our findings indicate that *Bhlha9* transiently regulates the expression of *Trp63* and its downstream genes in the AER and the progress zone during embryonic stages E10.5–E11.5, but not at later developmental stages.

Author Manuscript Author Manuscript Author Manuscript Author Manuscript

Limb development results from gradients of signaling molecules in three spatial dimensions: proximodigital, anteroposterior, and dorsoventral [22]. Specifically, for the development of the anteroposterior dimension, the AER contains a specialized cell cluster that expresses *TP63* (*Trp63*) and *Fgf8*. Failure to form the AER leads to a truncation of limb skeletal structures [23, 24]. The forelimbs of *Trp63*-knockout mice exhibit the abnormal expression of several genes, including *Fgf8*, and severe malformations such as a missing radius and autopod [5, 6]. It was also noted that mutations underlying SHFM4 exist in the *TP63* gene [3]. Therefore, *TP63* (*Trp63*) is thought to act as an AER maintenance gene. Similarly, *Fgf8* is also considered as an essential genes induced by *TP63* (*Trp63*) for AER structure [6, 25]. Cre-mediated inactivation of *Fgf8* in the early limb ectoderm resulted in a substantial reduction in limb bud size, a delay in *Shh* expression, dysregulation of *Fgf4* expression, and abnormalities in skeletal elements [26]. Furthermore, fibroblast growth factor (FGF) molecules, including FGF8, which is produced in the AER, suppress bone morphogenetic protein production in the interdigital tissue and act as inhibitors for the interdigital cell apoptosis [27]. Once the AER regresses, FGF production in the AER declines and bone morphogenetic protein (BMP) expression in the interdigital tissue is upregulated, leading to interdigital cell apoptosis [28–30]. Consequently, studies on the expression and maintenance of *TP63* (*Trp63*) and *Fgf8* are necessary to enhance our understanding of AER function, finger morphogenesis, and pathogenesis of SHFM and SHFLD.

Our investigation has revealed for the first time that disruption of *Bhlha9* expression in the progress zone leads to the upregulation and dysregulation of *Trp63* and *Fgf8* in the AER and the progress zone at E10.5 rather than at the interdigital cell apoptosis stage (Figs. 3, 4). Furthermore, the AER of the wild-type mouse had a characteristic convex structure, which was not clearly detected in *Bhlha9*-null limb buds. These observations indicate that *Bhlha9* expressed in the progress zone mainly contributes to the maintenance of AER formation by regulating *Trp63* expression in the AER and the progress zone at E10.5. This notion was corroborated by in vitro analysis, which included luciferase assays and qPCR (Fig. 5). A previous publication indicated that interdigital cell apoptosis was inhibited in *Bhlha9*-null limb [15]. Interdigital cell apoptosis normally occurs after AER regression [28–30]. Therefore, we speculated that cell death in the AER of *Bhlha9*-null limb buds is abnormal compared with that in wild-type mouse limb buds. However, no significant difference in AER cell death was found in *Bhlha9*-knockout mouse limb buds on the basis of Nile blue sulfate staining, which is used to detect apoptotic cells (Fig. S3). On the basis of previous reports and our finding of *Trp63* and *Fgf8* overexpression in *Bhlha9*-null limb buds, we suggest that abnormal AER formation and overexpression of *Fgf8*, which is an interdigital cell apoptosis inhibitor, induced by *Trp63* in the *Bhlha9*-null AER and progress zone inhibits interdigital cell apoptosis, but not AER regression, leading to the syndactyly (Fig. 6). Consequently, our observations suggest that abnormal expression of *Bhlha9* leads to SHFM and SHFLD via dysregulation of AER formation and associated gene expression.

Supplementary Material

Refer to Web version on PubMed Central for supplementary material.

Author Manuscript Author Manuscript Author Manuscript Author Manuscript

Acknowledgments

This work was supported by Core Research for the Evolutionary Science and Technology (CREST) funding from the Japan Science and Technology Agency (JST), AMED-CREST from the Japan Agency for Medical Research and Development (AMED), KAKENHI (Grant Numbers 26113008, 15H02560, and 15K15544) from the Japan Society for the Promotion of Science, Grants from the National Institutes of Health (Grant Numbers AR050631 and AR065379), the Naito Foundation, and a Bristol-Myers K.K. RA Clinical Investigation Grant to Hiroshi Asaha. The funders had no role in study design, data collection and analysis, the decision to publish the findings, or preparation of the manuscript. We thank Natsuko Izumi and Daiki Fukuchi for technical assistance.

References

1. Gurrieri F, Everman DB (2013) Clinical, genetic, and molecular aspects of split-hand/foot malformation: an update. Am J Med Genet A 11:2860–2872
2. Ianakiev P, Kilpatrick MW, Toudjarska I, Basel D, Beighton P, Tsipouras P (2000) Split-hand/split-foot malformation is caused by mutations in the p63 gene on 3q27. Am J Hum Genet 1:59–66
3. van Bokhoven H, Hamel BC, Bamshad M, Sangiorgi E, Gurrieri F et al. (2001) p63 gene mutations in EEC syndrome, limb-mammary syndrome, and isolated split hand-split foot malformation suggest a genotype-phenotype correlation. Am J Hum Genet 3:481–492
4. Yang A, Kaghad M, Wang Y, Gillett E, Fleming MD, Dotsch V, Andrews NC, Caput D, McKeon F (1998) p63, a p53 homolog at 3q27–29, encodes multiple products with transactivating, death-inducing, and dominant-negative activities. Mol Cell 3:305–316
5. Yang A, Schweitzer R, Sun D, Kaghad M, Walker N, Bronson RT, Tabin C, Sharpe A, Caput D, Crum C, McKeon F (1999) p63 is essential for regenerative proliferation in limb, craniofacial and epithelial development. Nature 6729:714–718
6. Mills AA, Zheng B, Wang XJ, Vogel H, Roop DR, Bradley A (1999) p63 is a p53 homologue required for limb and epidermal morphogenesis. Nature 6729:708–713
7. Baquero-Montoya C, Gil-Rodriguez MC, Hernandez-Marcos M, Teresa-Rodrigo ME, Vicente-Gabas A, Bernal ML, Casale CH, Bueno-Lozano G, Bueno-Martinez I, Queralt E, Villa O, Hernando-Davalillo C, Armengol L, Gomez-Puertas P, Puisac B, Selicorni A, Ramos FJ, Pie J (2014) Severe ipsilateral musculoskeletal involvement in a Cornelia de Lange patient with a novel NIPBL mutation. Eur J Med Genet 9:503–509
8. Capra V, Mirabelli-Badenier M, Stagnaro M, Rossi A, Tassano E, Gimelli S, Gimelli G (2012) Identification of a rare 17p13.3 duplication including the BHLHA9 and YWHAE genes in a family with developmental delay and behavioural problems. BMC Med Genet 13:93 [PubMed: 23035971]
9. Klopocki E, Lohan S, Doelken SC, Stricker S, Ockeloen CW et al. (2012) Duplications of BHLHA9 are associated with ectrodactyly and tibia hemimelia inherited in non-Mendelian fashion. J Med Genet 2:119–125
10. Luk HM, Wong VC, Lo IF, Chan KY, Lau ET, Kan AS, Tang MH, Tang WF, She WM, Chu YW, Sin WK, Chung BH (2014) A prenatal case of split-hand malformation associated with 17p13.3 triplication—a dilemma in genetic counseling. Eur J Med Genet 2–3:81–84
11. Nagata E, Kano H, Kato F, Yamaguchi R, Nakashima S et al. (2014) Japanese founder duplications/triplications involving BHLHA9 are associated with split-hand/foot malformation with or without long bone deficiency and Gollop-Wolfgang complex. Orphanet J Rare Dis doi: 10.1186/s13023-014-0125-5
12. Nagata E, Haga N, Fujisawa Y, Fukami M, Nishimura G, Ogata T (2015) Femoral-tibial-digital malformations in a boy with the Japanese founder triplication of BHLHA9. Am J Med Genet A 12:3226–3228
13. Petit F, Andrieux J, Demeer B, Collet LM, Copin H, Boudry-Labis E, Escande F, Manouvrier-Hanu S, Mathieu-Dramard M (2013) Split-hand/foot malformation with long-bone deficiency and BHLHA9 duplication: two cases and expansion of the phenotype to radial agenesis. Eur J Med Genet 2:88–92
14. Petit F, Jourdain AS, Andrieux J, Baujat G, Baumann C, Beneteau C, David A, Faivre L, Gaillard D, Gilbert-Dussardier B, Jouk PS, Le Caignec C, Loget P, Pasquier L, Porchet N, Holder-

Author Manuscript Author Manuscript Author Manuscript Author Manuscript

Espinasse M, Manouvrier-Hanu S, Escande F (2014) Split hand/foot malformation with long-bone deficiency and BHLHA9 duplication: report of 13 new families. Clin Genet 5:464–469

15. Schatz O, Langer E, Ben-Arie N (2014) Gene dosage of the transcription factor fingerin (bHLHA9) affects digit development and links syndactyly to ectrodactyly. Hum Mol Genet 20:5394–5401
16. Malik S, Percin FE, Bornholdt D, Albrecht B, Percesepe A, Koch MC, Landi A, Fritz B, Khan R, Mumtaz S, Akarsu NA, Grzeschik KH (2014) Mutations affecting the BHLHA9 DNA binding domain cause MSSD, mesoaxial synostotic syndactyly with phalangeal reduction, Malik–Percin type. Am J Hum Genet 6:649–659
17. Yokoyama S, Hashimoto M, Shimizu H, Ueno-Kudoh H, Uchibe K, Kimura I, Asahara H (2008) Dynamic gene expression of Lin28 during embryonic development in mouse and chicken. Gene Expr Patterns 3:155–160
18. Miyaki S, Sato T, Inoue A, Otsuki S, Ito Y, Yokoyama S, Kato Y, Takemoto F, Nakasa T, Yamashita S, Takada S, Lotz MK, Ueno-Kudo H, Asahara H (2010) MicroRNA-140 plays dual roles in both cartilage development and homeostasis. Genes Dev 11:1173–1185
19. Moon AM, Capecchi MR (2000) Fgf8 is required for outgrowth and patterning of the limbs. Nat Genet 4:455–459
20. Mahmood R, Bresnick J, Hornbruch A, Mahony C, Morton N, Colquhoun K, Martin P, Lumsden A, Dickson C, Mason I (1995) A role for FGF-8 in the initiation and maintenance of vertebrate limb bud outgrowth. Curr Biol 7:797–806
21. Casanova JC, Uribe V, Badia-Careaga C, Giovinazzo G, Torres M, Sanz-Ezquerro JJ (2011) Apical ectodermal ridge morphogenesis in limb development is controlled by Arid3b-mediated regulation of cell movements. Development 6:1195–1205
22. Zeller R, Lopez-Rios J, Zuniga A (2009) Vertebrate limb bud development: moving towards integrative analysis of organogenesis. Nat Rev Genet 12:845–858
23. Saunders JW, Jr (1948) The proximo-distal sequence of origin of the parts of the chick wing and the role of the ectoderm. J Exp Zool 3:363–403
24. Summerbell D (1974) A quantitative analysis of the effect of excision of the AER from the chick limb-bud. J Embryol Exp Morphol 3:651–660
25. Guerrini L, Costanzo A, Merlo GR (2011) A symphony of regulations centered on p63 to control development of ectoderm-derived structures. J Biomed Biotechnol 2011:864904 [PubMed: 21716671]
26. Lewandoski M, Sun X, Martin GR (2000) Fgf8 signalling from the AER is essential for normal limb development. Nat Genet 4:460–463
27. Pajni-Underwood S, Wilson CP, Elder C, Mishina Y, Lewandoski M (2007) BMP signals control limb bud interdigital programmed cell death by regulating FGF signaling. Development 12:2359–2368
28. Guha U, Gomes WA, Kobayashi T, Pestell RG, Kessler JA (2002) In vivo evidence that BMP signaling is necessary for apoptosis in the mouse limb. Dev Biol 1:108–120
29. Ganan Y, Macias D, Duterque-Coquillaud M, Ros MA, Hurle JM (1996) Role of TGF beta s and BMPs as signals controlling the position of the digits and the areas of interdigital cell death in the developing chick limb autopod. Development 8:2349–2357
30. Merino R, Rodriguez-Leon J, Macias D, Ganan Y, Economides AN, Hurle JM (1999) The BMP antagonist gremlin regulates outgrowth, chondrogenesis and programmed cell death in the developing limb. Development 23:5515–5522

Author Manuscript Author Manuscript Author Manuscript Author Manuscript

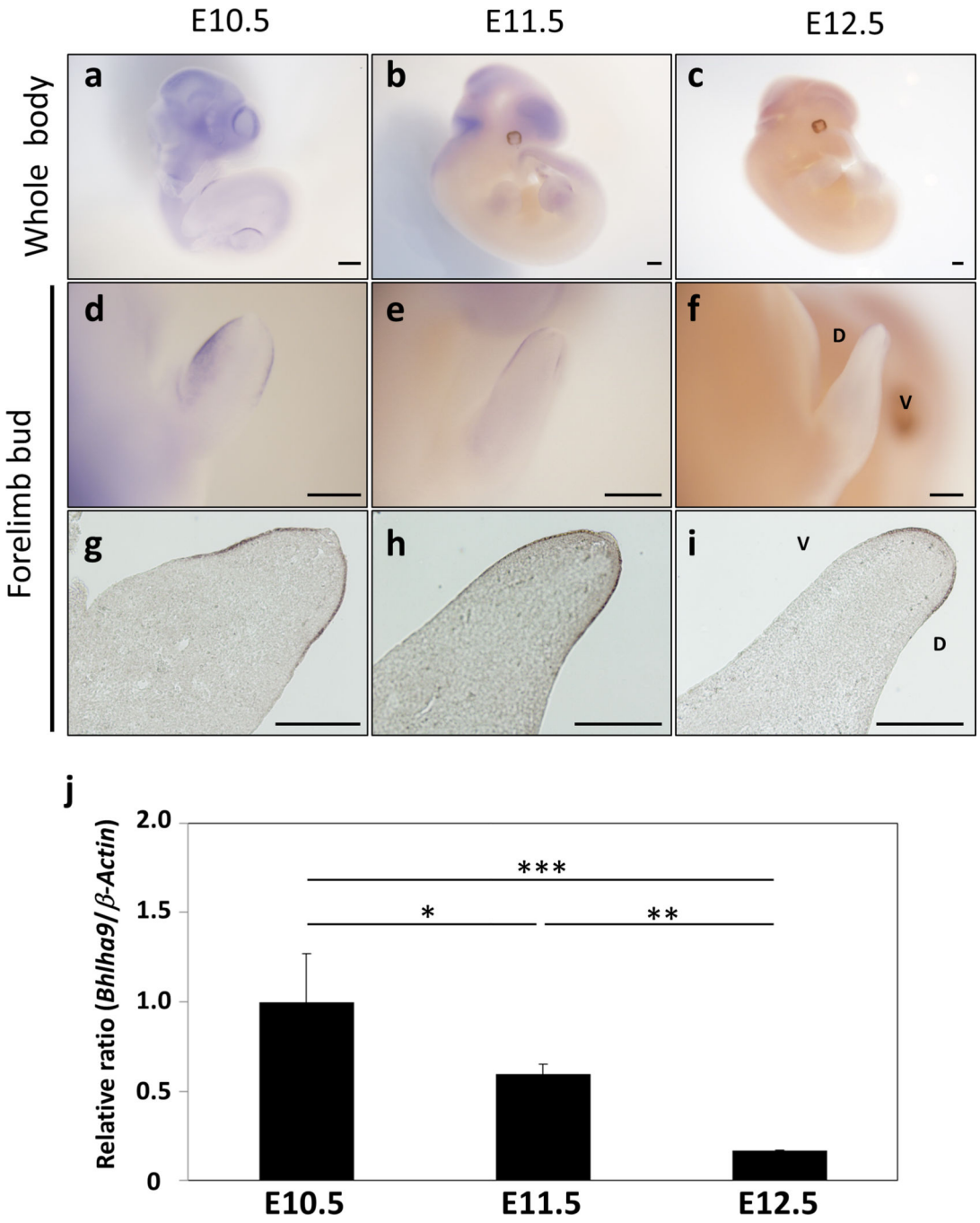

Fig. 1. *Bhlha9* is expressed in the limb ectoderm.

Bhlha9 is expressed on both the dorsal side and the ventral side of the autopod in wild-type mouse limb buds at embryonic day 10.5 (*E10.5*) and embryonic day (*E11.5*), as assessed by whole-mount in situ hybridization (*a–f*). Although *Bhlha9* expression in the limb at embryonic day 12.5 (*E12.5*) was unclear from whole-mount in situ hybridization, it was detectable in the longitudinal section of wild-type forelimbs at each stage (*g–i*). Expression of *Bhlha9* relative to β-*Actin* in E10.5–E12.5 wild-type or *Bhlha9*-knockout whole limb buds was assessed by quantitative real-time PCR (*j*) The relative ratios against E10.5 limb

RNA (set to 1.0) are presented as the mean ± standard deviation ($n = 4$). *Asterisks* represent a statistically significant difference on the basis of Tukey's test (*one asterisk* $p < 0.05$, *two asterisks* $p < 0.01$, *three asterisks* $p < 0.001$). *D* dorsal, *V* ventral. *Scale bar* 200 μm

Author Manuscript Author Manuscript Author Manuscript Author Manuscript

Author Manuscript Author Manuscript Author Manuscript Author Manuscript

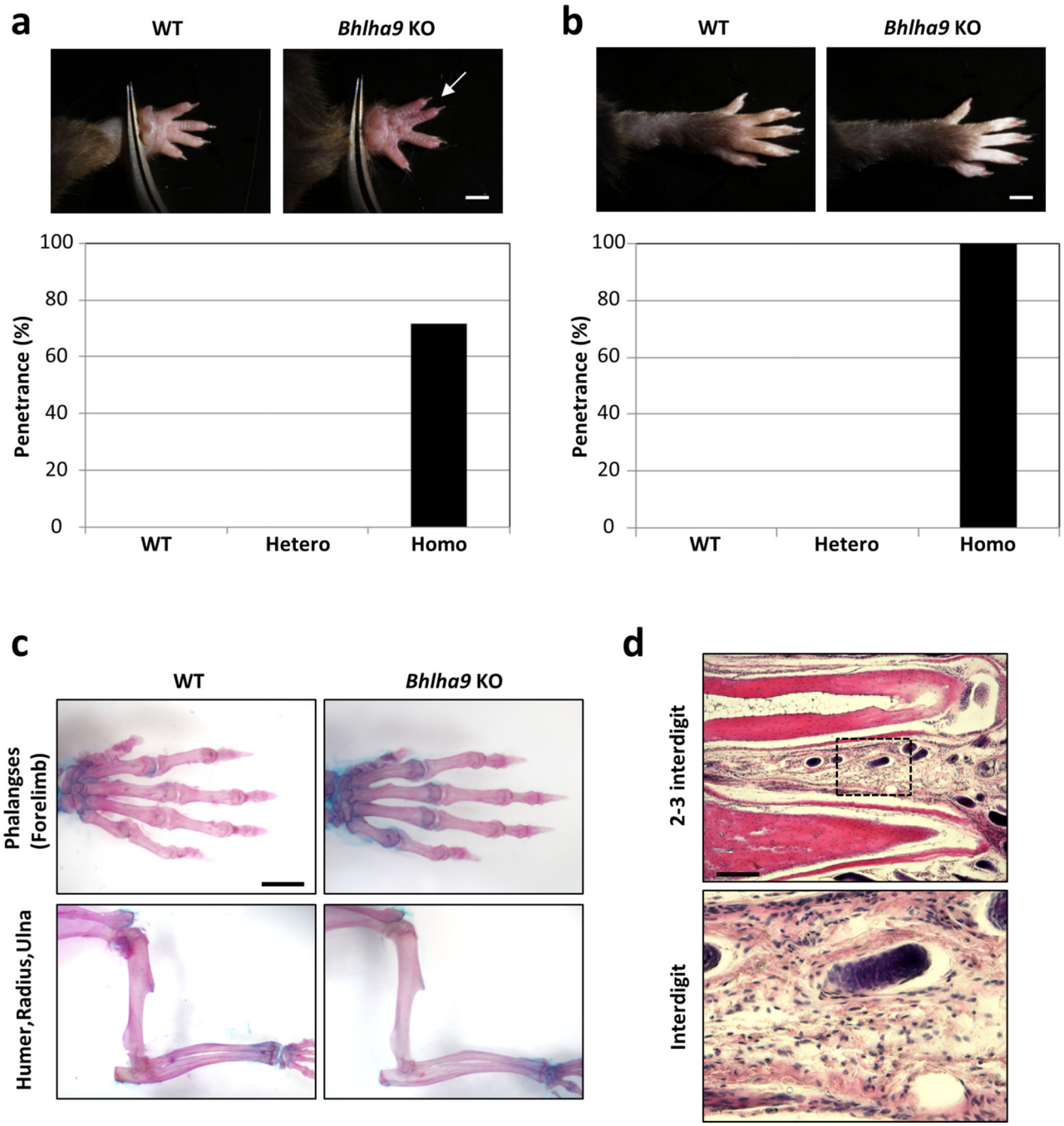

Fig. 2. Phenotype of *Bhlha9*-knockout mice.

a The appearance of the forelimb in 3-month-old wild-type and *Bhlha9*-knockout mice. Various degrees of syndactyly were observed in the forelimbs of *Bhlha9*-knockout mice. A white arrow indicates interdigital webbing. Most *Bhlha9*-knockout mice (71.79%) had a webbed digit in the forelimb ($n = 39$). **b** The appearance of the hindlimb in 3-month-old wild-type and *Bhlha9*-knockout mice. All *Bhlha9*-knockout mice displayed poliosis in the hindlimbs ($n = 17$). **c** Skeletal staining of the forelimbs of 3-month-old wild-type and *Bhlha9*-knockout mice. Limbs were dissected from 3-month-old wild-type and *Bhlha9*-

Author Manuscript Author Manuscript Author Manuscript Author Manuscript

knockout mice and bone and cartridge were stained by alizarin red and alcian blue, respectively. In *Bhlha9*-knockout mice, no anomalies in humerus, radius, ulna, or forelimb phalange length were detected. **d** Hematoxylin and eosin staining of the interdigital webbing in adult *Bhlha9*-knockout mice. Longitudinal sections of interdigit 2–3 in 3-month-old adult *Bhlha9*-knockout mouse forelimbs were stained by hematoxylin and eosin. Staining revealed remaining cells and eosinophilic fibers in the interdigital region. The *lower panel* shows a higher magnification of the region marked in the *upper panel*. *KO* knockout, *WT* wild type. *Scale bar* **a**, **b** 1 mm, **c**, **d** 200 μm.

Author Manuscript Author Manuscript Author Manuscript Author Manuscript

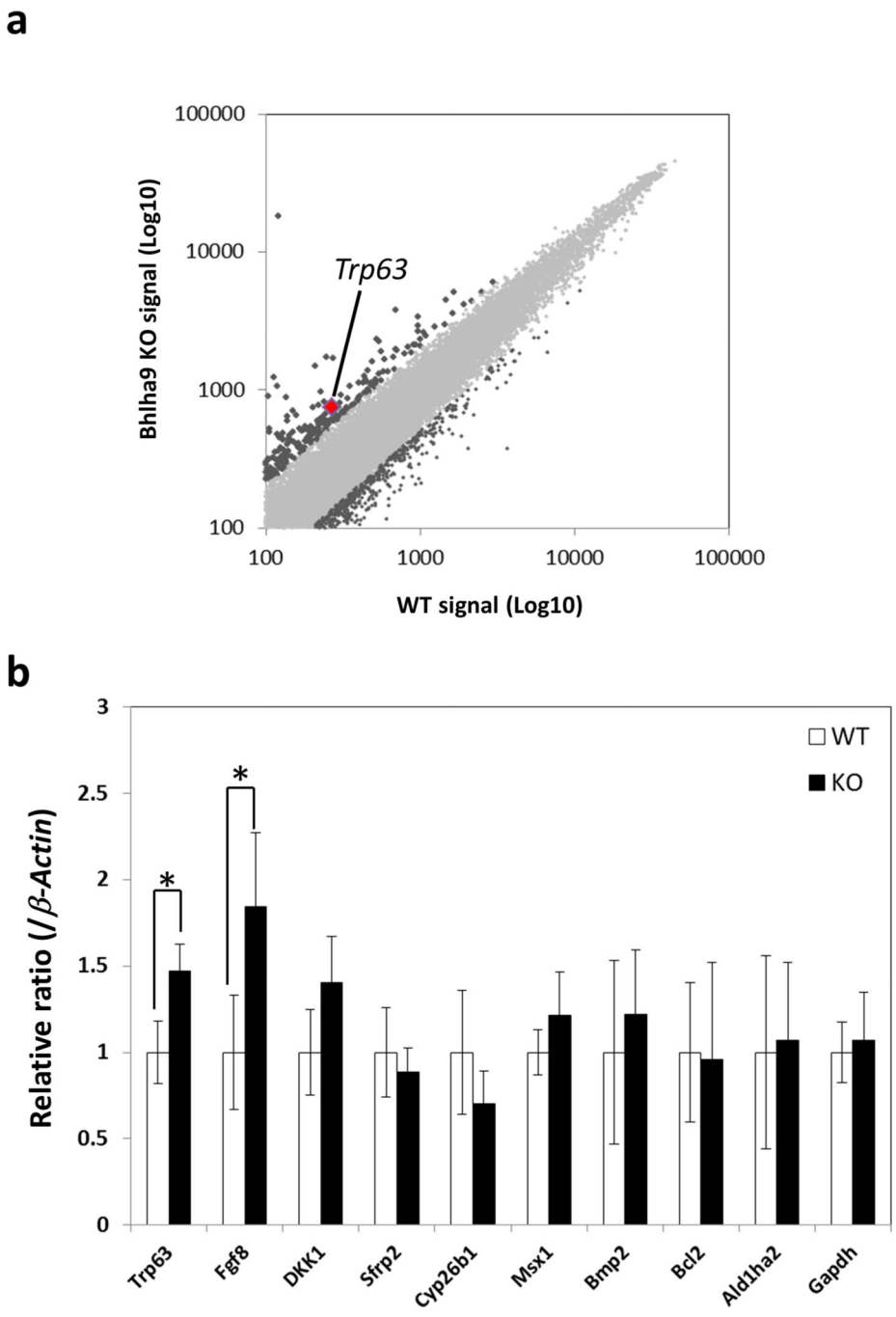

Fig. 3. *Trp63* and *Fgf8* expression is upregulated in *Bhlha9*-knockout mouse limb buds.

a The GeneChip signal value of embryonic day 10.5 (E10.5) *Bhlha9*-knockout mouse limb bud RNA compared to E10.5 wild-type mouse limb bud RNA as a scatter plot ($n = 1$, $R2 = 0.9717$). The signal value of *Trp63* (wild type 269, knockout 742) is shown by a *red dot*. Differentially expressed genes are shown in *dark gray* (fold change greater than 2). **b** Expression of various syndactyly-associated genes in *Bhlha9*-knockout mouse limbs. Expression of selected genes relative to β-*Actin* expression in E10.5 wild-type or *Bhlha9*-knockout mouse whole limb buds was assessed by quantitative real-time PCR. The relative

ratios against E10.5 wild- type mouse limb RNA (set to 1.0) are presented as the mean ± standard deviation ($n = 4$). An *asterisk* represents statistical significance ($p < 0.05$), as assessed by Student's *t* test. *KO* knockout, *WT* wild type

Author Manuscript Author Manuscript Author Manuscript Author Manuscript

Author Manuscript
Author Manuscript
Author Manuscript
Author Manuscript

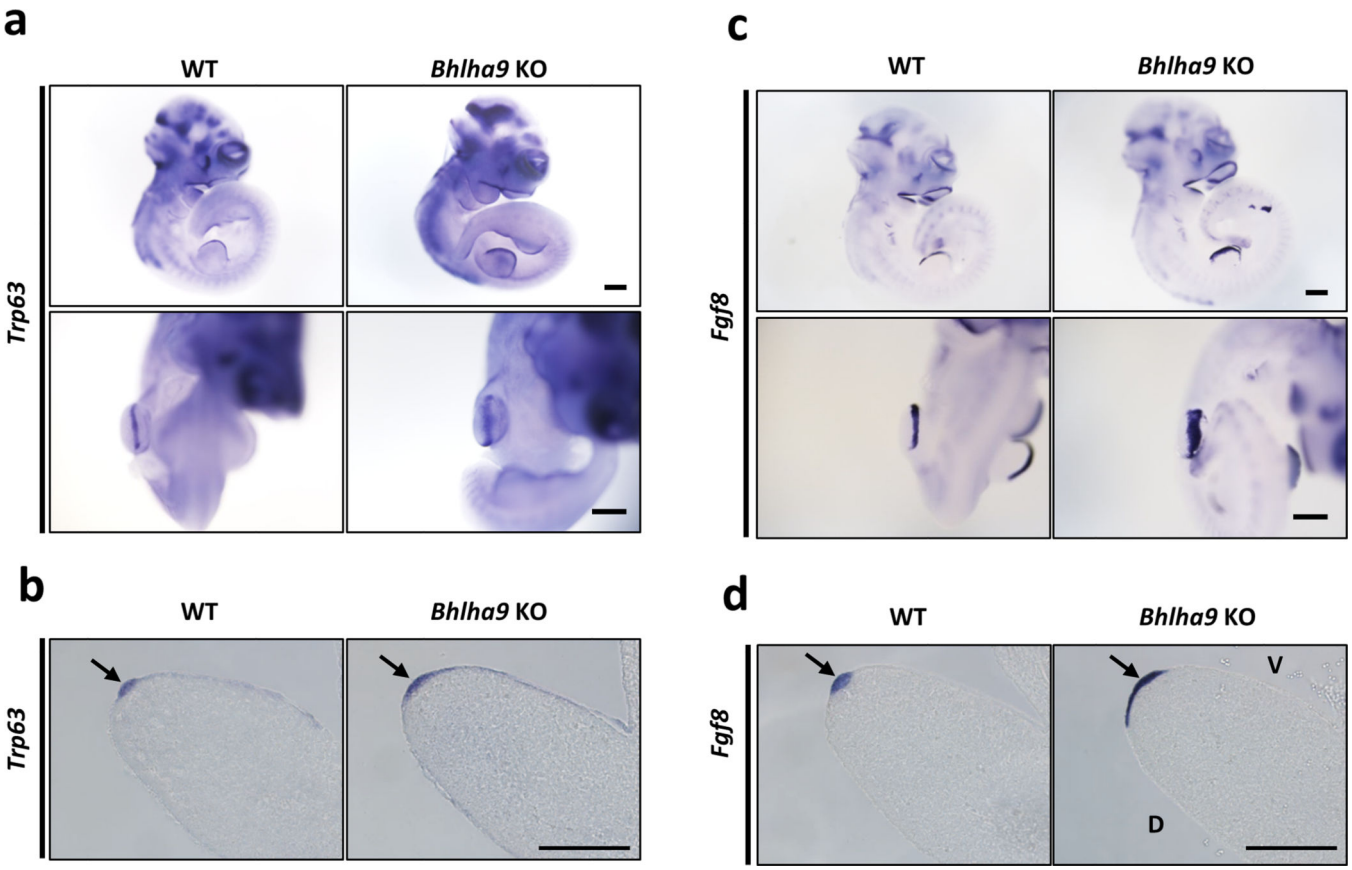

Fig. 4. *Bhlha9* contributes to apical ectodermal ridge (AER) formation.

Expression patterns of *Trp63* and *Fgf8* in embryonic day 10.5 wild-type and *Bhlha9*-knockout mouse limb buds. For confirmation of the real-time PCR results, wherein *Trp63* and *Fgf8* expression was increased in *Bhlha9*-knockout mouse limb buds, the expression pattern of each gene was detected by whole-mount in situ hybridization (**a**, **b**). Whole-mount in situ hybridization using embryo limb buds also showed the expansion of each gene's expression region in the limb ectoderm (**c**, **d**). *Arrows* indicate the AER structure. *D* dorsal, *KO* knockout, *V* ventral, *WT* wild-type. *Scale bar* 200 μm

Author Manuscript Author Manuscript Author Manuscript Author Manuscript

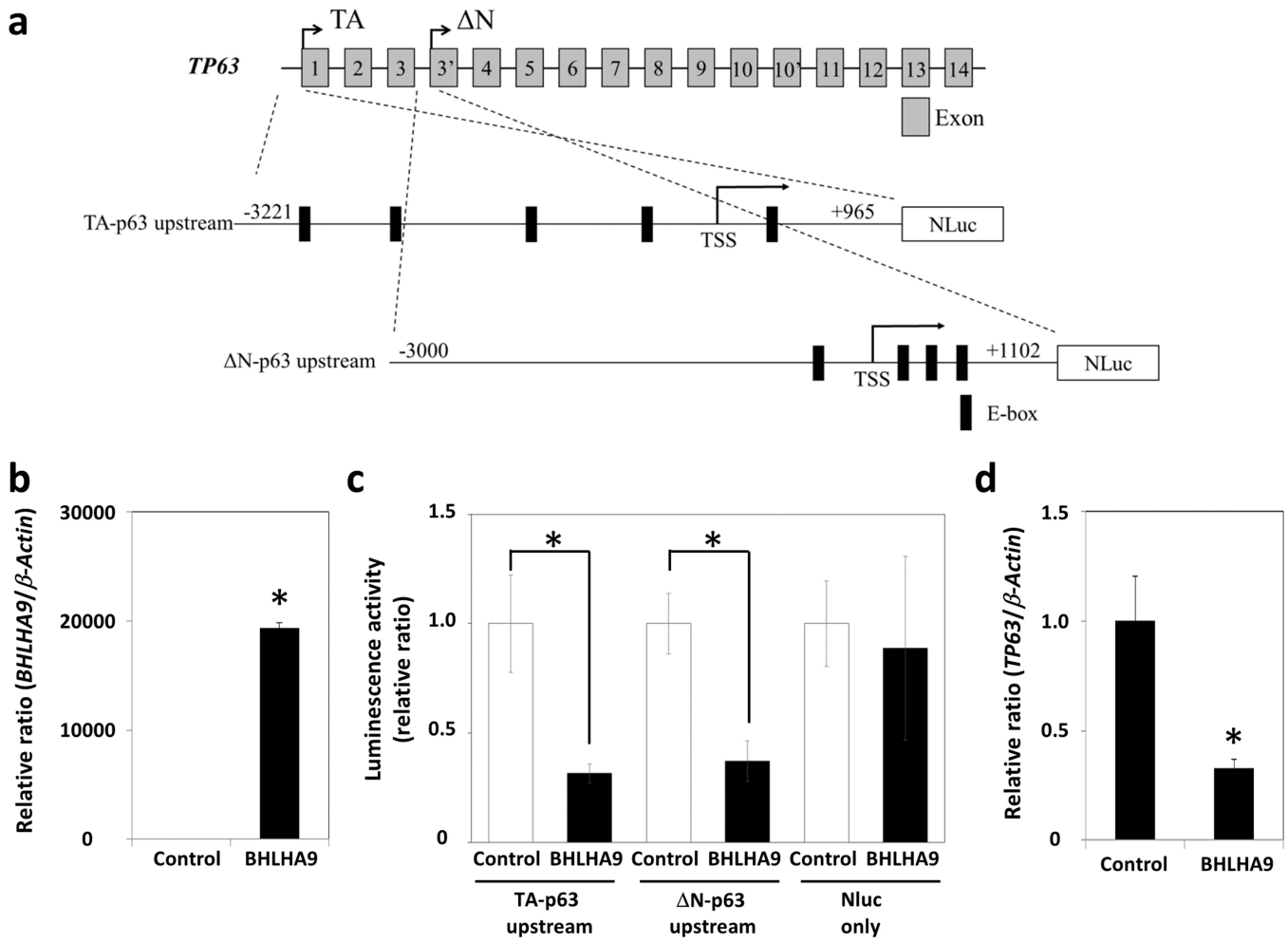

Fig. 5. *BHLHA9* directly regulates *TP63* expression.

a Transactivating TP63 (*TA-p63*) and nontransactivating TP63 (Δ*N-p63*) promoter driven luciferase reporter gene constructs. Each 4-kb upstream fragment from the first protein coding exon of TA-*p63* and ΔN-*p63* was selected and cloned into a nanoluciferase (*NLuc*) vector. **b**, **c** Luciferase assay using 3×FLAG-BHLHA9-expressing HeLa stable cells. HeLa stable cells were transfected with TA-*p63* and ΔN-*p63* promoter driven luciferase reporter constructs for luciferase assays. 3×FLAG-BHLHA9 overexpression against control HeLa stable cells (set to 1.0) was sufficiently detected on the basis of in vitro analysis (**b**) ($n = 4$). The relative ratio of each *TP63*-promoter-driven luciferase activity against control HeLa stable cells (set to 1.0) is presented as the mean ± standard deviation ($n = 4$). The luciferase activity significantly reduced with the overexpression of 3×FLAG-BHLHA9 (**c**). An *asterisk* represents statistical significance ($p < 0.05$) as assessed by Student's *t* test. **d** Endogenous *TP63* expression in 3×FLAG-BHLHA9-expressing HeLa cells. Expression of *TP63*, including TA-*p63* and ΔN-*p63*, relative to that of β-*Actin* in control HeLa cells or 3×FLAG-BHLHA9-expressing HeLa cells was assessed by quantitative real-time PCR. The relative ratios against control cells (set to 1.0) are presented as the mean ± standard deviation ($n = 4$). An *asterisk* represents statistical significance ($p < 0.05$), as assessed by Student's *t* test. *TSS* transcription start site

Author Manuscript Author Manuscript Author Manuscript Author Manuscript

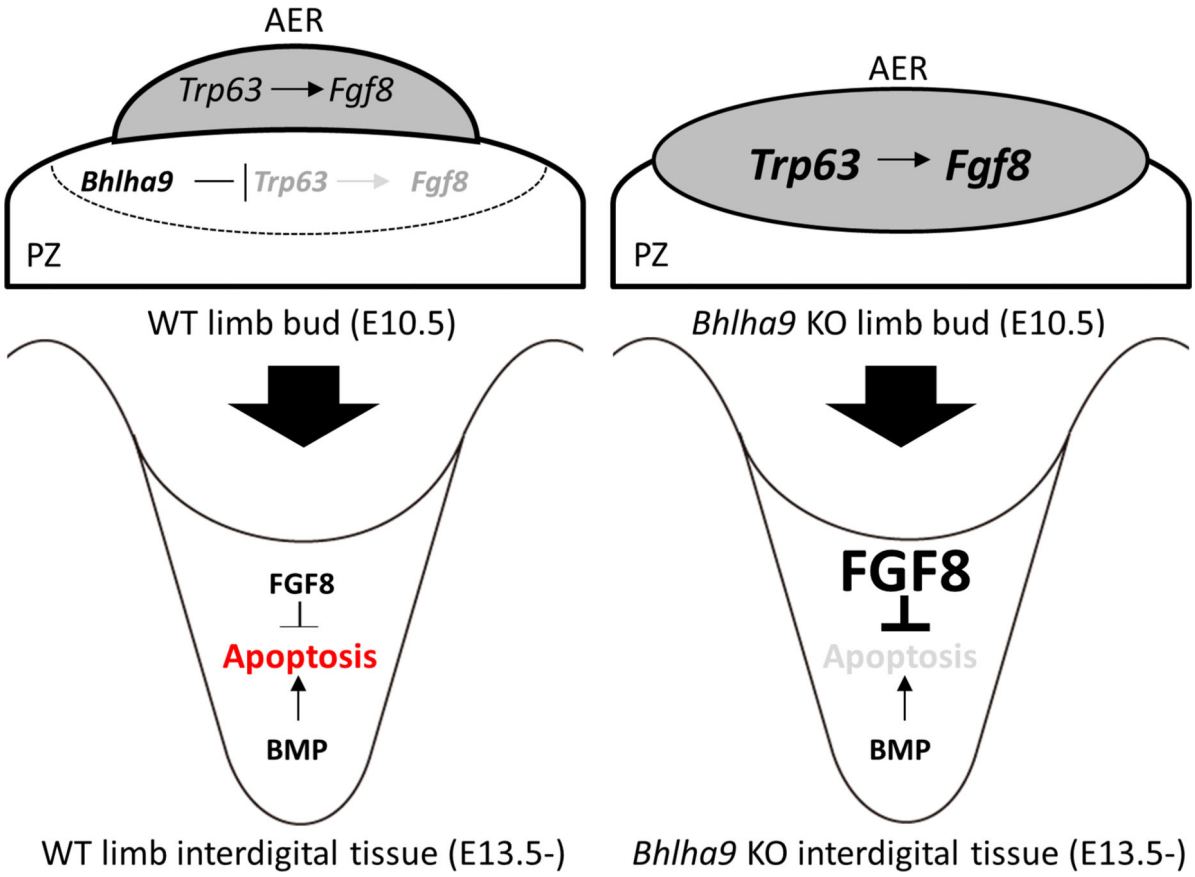

Fig. 6. *Bhlha9*-knockout mouse limb buds.

In the wild-type mouse limb bud, *Trp63* and *Fgf8* are expressed in the apical ectodermal ridge (*AER*), and this structure exhibits a characteristic convex shape. However, *Trp63* and *Fgf8* are overexpressed and dysregulated in *Bhlha9*-null AERs and progress zones via aberrant regulation of *Trp63* expression by *Bhlha9*. Consequently, overexpression of fibroblast growth factor 8 (*FGF8*) in *Bhlha9*-knockout mouse limbs inhibits interdigital cell apoptosis, leading to the syndactyly. *BMP* bone morphogenetic protein, *E* embryonic day, *KO* knockout, *PZ* progress zone, *WT* wild type